有机化学 DOI: 10.6023/cjoc202210011 研究论文
Chinese Journal of Organic Chemistry ARTICLE

大 Stokes 位移的近红外氟硼二吡咯(BODIPY)荧光探针应用于生物体中 $Na_2S_2O_4$ 的检测

赵小龙*,[a] 郭亮武[a] 李宇晴[a] 冉启元[a] 吴会慧[a] 张 祯[a]
苏瀛鹏[a] 周鹏鑫[a] 燕 娜[b]
([a]西北师范大学化学化工学院 教育部生态环境相关高分子重点实验室 兰州 730070)
([b]兰州大学药学院 兰州 730000)

摘要 基于氟硼二吡咯(BODIPY)的骨架结构, 设计合成了两种近红外荧光探针 **Azo-BDP1** 和 **Azo-BDP2**, 其 Stokes 位移分别为 217 和 224 nm. 作为 $Na_2S_2O_4$ 的两个可视化探针, **Azo-BDP1** 和 **Azo-BDP2** 具有高灵敏度和高选择性. 机理研究方面, 采用质谱分析证实了识别机制. 除此之外, 探索了 **Azo-BDP1** 在生物体中 $Na_2S_2O_4$ 的荧光成像.
关键词 氟硼二吡咯(BODIPY); 大斯托克斯位移; 可视化; 近红外; $Na_2S_2O_4$

Near-Infrared Visualization Fluoroboron Dipyrrole (BODIPY) Fluorescent Probe with Large Stokes Shift for Detecting $Na_2S_2O_4$ *in vivo*

Zhao, Xiaolong*,[a] Guo, Liangwu[a] Li, Yuqing[a] Ran, Qiyuan[a] Wu, Huihui[a]
Zhang, Zhen[a] Su, Yingpeng[a] Zhou, Pengxin[a] Yan, Na[b]
([a] *Laboratory of Eco-Environment-Related Polymer Materials*, *Ministry of Education*, *College of Chemistry and Chemical Engineering*, *Northwest Normal University*, *Lanzhou 730070*)
([b] *School of Pharmacy*, *Lanzhou University*, *Lanzhou 730000*)

Abstract Based on the main skeleton of fluoroboron dipyrrole (BODIPY), two near-infrared fluorescent probes **Azo-BDP1** and **Azo-BDP2** were rationally designed and synthesized with large Stokes shift of 217 and 224 nm, respectively. As two visualized probes for $Na_2S_2O_4$, **Azo-BDP1** and **Azo-BDP2** exhibited high sensitivity and selectivity. The reaction-based recognition mechanism was confirmed by mass spectral analysis, in addition, fluorescence imaging studies in zebrafish embryos and zebrafish proved that the probe **Azo-BDP1** is suitable for the detection of $Na_2S_2O_4$ *in vivo*.
Keywords fluoroboron dipyrrole (BODIPY); large Stokes shift; visualization; near-infrared; $Na_2S_2O_4$

1 Introduction

Sodium dithionite ($Na_2S_2O_4$), commonly known for its reducing properties, was widely used in the textile industry for the purpose of reductive dyeing, reduction cleaning, bleaching, organic synthesis, wood pulp and papermaking, *etc.*[1] It is also regarded as a food-grade product preservative, bleaching agent, and antioxidant.[2] Moreover, as a simulate of azo reductase (AzoR) which is defined as a marker for the construction of fluorescent probes for tumor hypoxia response,[3] $Na_2S_2O_4$ plays a critical role in assessing hypoxia-induced azo reduction and breakage.[4] It has been used by many scientific to imaging hypoxia tumor.[5-7] However, $Na_2S_2O_4$ is irritating to eyes, respiratory tract and skin, and can cause headache, nausea and vomiting after contact.[8] The conventional detection methods of sodium hydrosulfite include discoloration test, iodometry, capillary zone electrophoresis (CZE) and oxygen absorption as well as fluorescence analysis. In contrast, such fluorescent probe detection possesses several advantages involving high sensitivity, short response, and simple operation.[9] At the same time, fluorescent probe with large Stokes shifts has the advantages of small background interference, small sample damage, strong penetration, and high detection

* Corresponding author. E-mail: zhaoxl82@nwnu.edu.cn
Received October 14, 2022; revised March 10, 2023; published online March 23, 2023.
Project supported by the Gansu Province Industrial Support Program for Colleges (No. 2021CYZC-17), the Natural Science Foundation of Gansu Province (No. 21JR1RA227), and the National Natural Science Foundation of China (No. 21462039).
甘肃省高等学校产业支撑计划(No. 2021CYZC-17)、甘肃省自然科学基金(No. 21JR1RA227)、国家自然科学基金(No. 21462039)资助项目.

sensitivity.[11] Therefore, it is extremely necessary to develop a new type of multifunctional $Na_2S_2O_4$ fluorescence sensor.

In recent years, the detection of sulfur-containing substances by small molecule fluorescent probes has fascinated an increasing amount of attention.[12-15] Until now, several methods about monitoring $Na_2S_2O_4$ compounds have been reported with high selectivity and sensitivity,[16-18] while there is few or no molecular displaying near-infrared emission wavelengths and large Stokes shift. The large Stokes shift fluorescent dye possesses favorable advantages including low background interference, low light damage to biological samples,[19] strong sample penetration, high detection sensitivity and so on.[20-21] Boron-dipyrromethene (BODIPY) derivatives, with significant features such as high fluorescence quantum yield, high extinction coefficient, excellent photochemical stability and low biotoxicity,[22] have been extensively applied in potential sensors,[23] labeling material[24] and dye-sensitized solar cells (DSSCs).[25-26] Moreover, in the realm of biomarkers, BODIPY dyes also have broad application prospects in the detection of small biomolecules and bioimaging.[27-30] However, due to the structural feature of main skeleton of BODIPY, there are two factors restricting the development of efficient BODIPY probe for $Na_2S_2O_4$. On the one hand, the emission wavelength of normal BODIPY is less than 600 nm, on the other hand, the Stokes shift of BODIPY molecules is relatively small[31] (usually below 15 nm). In view of this, developing BODIPY fluorescent probes with deep-near infrared and large Stokes shift is regarded as promising strategy to detecting $Na_2S_2O_4$.

Herein, we report two near-infrared BODIPY fluorescent probes with large Stokes shifts aiming at developing a specific method for the detection of $Na_2S_2O_4$. Fluorescent probes suitable for $Na_2S_2O_4$ detection in living cells should fulfill definite requirements, such as near-infrared optical window, fluorescence enhancement, sensitive response and good selectivity. Therefore, in order to reasonably design the structure of the probe, several main aspects need to be considered. Meanwhile, the fluorescence probe for $Na_2S_2O_4$ should include a detection part and a fluorescence response one. In this work, the detection part was azo group and the fluorescence response section was the main skeleton of BODIPY, which two parts were connected together with a styrene group to form a conjugate structure.[32] In addition, considering the reaction activity of BODIPY at 2-, 6-positions caused by enhanced electron cloud density, two ester groups are introduced at these two sites to avoid the electrophilic reactions by electronic effect. Subsequently, the 2-thiophene substituents occupy the 8-position while the two methyl groups occupy at the 1-, 7-positions, which together limit the free rotation of the BODIPY skeleton, enhancing the Stokes shift significantly.[33] Driven by achieving deep-near infrared emission, the other two methyl groups are introduced in 3-, 5-positions in order to enlarge the conjugated styrene systems by Knoevenagel condensation.[34-35] It is worth noting that azobenzene derivatives is beneficial for the detection of $Na_2S_2O_4$ aiming at the azo bond for utilizing the reducing properties of the $Na_2S_2O_4$.

2 Results and discussion

2.1 Probe design and synthesis

As show in Scheme 1, BODIPY derivatives **Azo-BDP1** and **Azo-BDP2** were designed and prepared by the Knoevenagel condensation reaction, fitting azobenzene as a fluorescence quencher onto the BODIPY core. This method has been proven feasible to reaction with 3,5-dimethyl-BODIPY dyes.[36-37] The phenyl groups on the 3,5-positions of BODIPY could not only cause the wavelength red shift, but also enlarge the Stokes shift.[27]

Thus, the probe was synthesized according to Scheme 1. **Ab** which was synthesized from *p*-nitrobenzaldehyde by reduction with reduced iron powder, was further coupled with phenol to yield **Azo1**. The **Azo1** was protected with chloromethyl methyl ether (MOMCl) to give **Azo2** followed by preparing **BDP** with pyrrole derivatives and 2-thiophenecarboxaldehyde in a one-pot reaction.[36] **BDP** and **Azo** were transformed into **Azo-BDP1** and **Azo-BDP2** by Knoevenagel condensation reaction. All compounds were characterized by ^{1}H NMR, ^{13}C NMR and ESI-MS. Then **Azo-BDP1** and **Azo-BDP2** were utilized for the specific detection of $Na_2S_2O_4$, as a result, a turn-on fluorescent response was obtained, which leads to the development of a highly sensitive and selective method for $Na_2S_2O_4$ in living cells.

2.2 Spectra response properties to **Azo-BDP1** and **Azo-BDP2**

With **Azo-BDP1** and **Azo-BDP2** in hand, their optical responses to $Na_2S_2O_4$ were first assessed by ultraviolet-visible absorption spectroscopy and fluorescence spectroscopy. There are two strong absorption peaks located at around 585 and 592 nm, respectively. After addition of $Na_2S_2O_4$, the absorption peaks at 585 and 590 nm almost disappear, while two new blue shift absorption peaks appeare at 485 and 492 nm. Along with obvious color change, the probe **Azo-BDP1** turns from blue to pink and **Azo-BDP2** from purple to pink. These colors variability indicates that **Azo-BDP1** and **Azo-BDP2** can serve as a sensitive ''naked-eye'' indicator for $Na_2S_2O_4$. Impressively, after constantly adding $Na_2S_2O_4$ to the **Azo-BDP1** and **Azo-BDP2** solution separately, the fluorescence turn-on response was extremely obvious. Under the irradiation of 365 nm ultraviolet lamp, the solution emits strong red fluorescence (inset of Figure 1). As shown in Figure 1a, the fluorescence intensity at 685 nm gradually increased to 10-fold along with the stepwise addition of 130 μmol/L $Na_2S_2O_4$. In this process, **Azo-BDP1** exhibits a large Stokes shift of 217 nm. Similarly, after treatment with $Na_2S_2O_4$, the fluorescence intensity of **Azo-BDP2** was significantly enhanced at 692 nm, which increased 11-fold with the Stokes shift of 224 nm (Figure 1c). Furthermore, the fluorescence intensities of **Azo-BDP1** at 685 nm (I_{685}) and **Azo-BDP2** at 692 nm (I_{692}) demonstrate an outstanding linear relationship

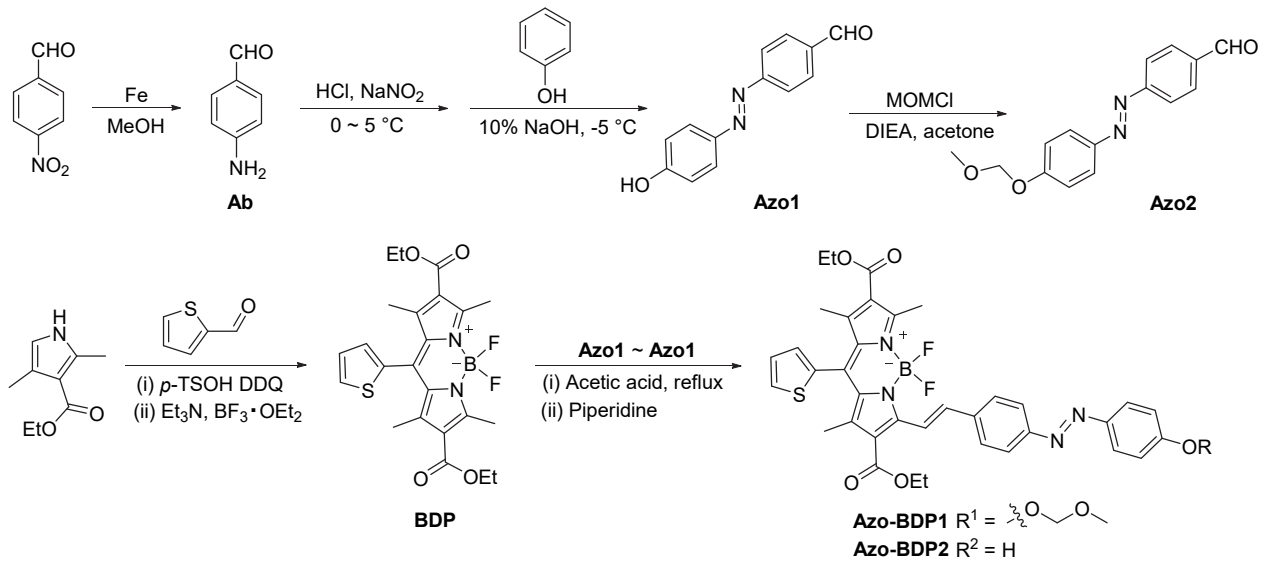

Scheme 1 Synthesis route of **Azo-BDP1** and **Azo-BDP2**

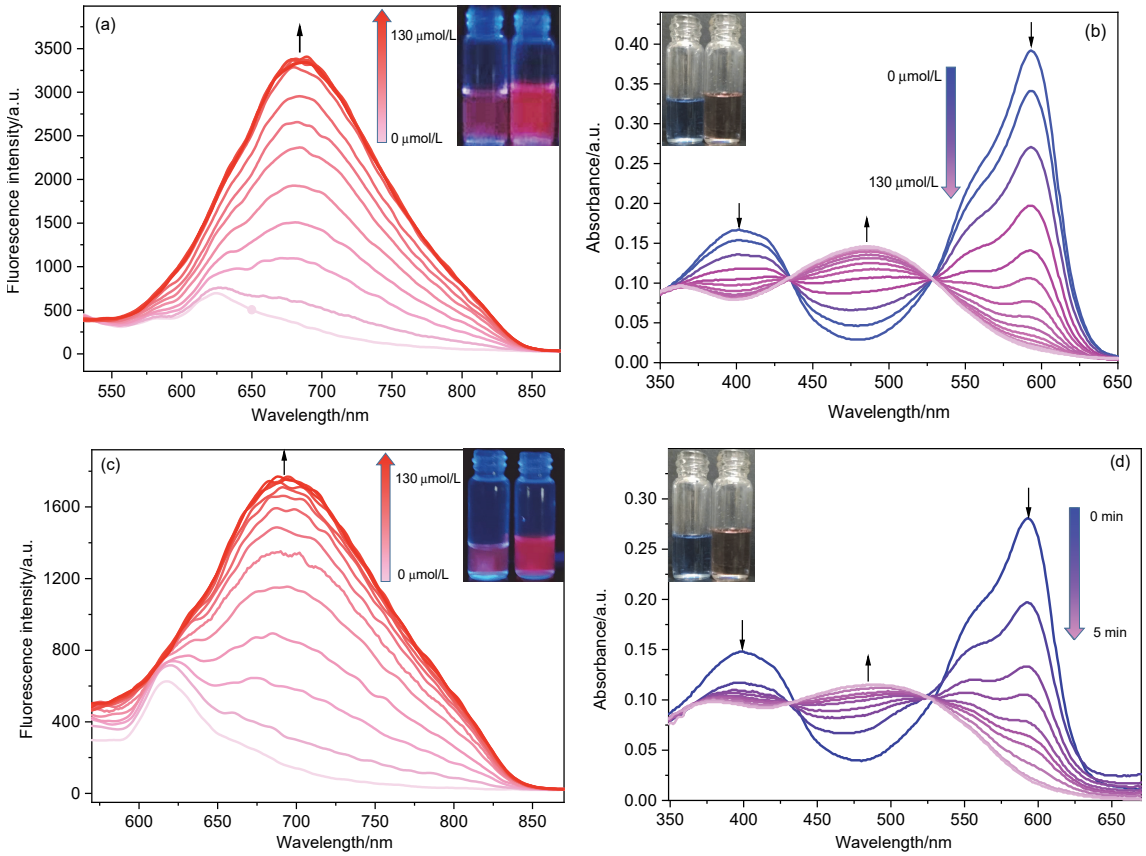

Figure 1 (a) Fluorescence emission spectra of 10 μmol/L **Azo-BDP1** upon additional different concentrations of $Na_2S_2O_4$ (0～130 μmol/L) in dimethyl sulfoxide (DMSO) solution (inset: color change of **Azo-BDP1** in the absence (left) or presence (right) of 100 μmol/L $Na_2S_2O_4$ under irradiation at 365 nm); (b) UV-vis absorption of **Azo-BDP1** upon additional different concentrations of $Na_2S_2O_4$ (0～130 μmol/L) in DMSO solution (inset: images of **Azo-BDP1** in the absence (left) or presence (right) of 100 μmol/L $Na_2S_2O_4$ under naked eye colorimetric changes); (c) Fluorescence emission spectra of 10 μmol/L **Azo-BDP1** upon additional different concentrations of $Na_2S_2O_4$ (0～130 μmol/L) in DMSO solution (inset: color change of **Azo-BDP2** in the absence (left) or presence (right) of 100 μmol/L $Na_2S_2O_4$ under irradiation at 365 nm); (d) UV-vis absorption of **Azo-BDP2** upon additional different concentrations of $Na_2S_2O_4$ (0～130 μmol/L) in DMSO solution (inset: images of **Azo-BDP2** in the absence (left) or presence (right) of 100 μmol/L $Na_2S_2O_4$ under naked eye colorimetric changes)

Error bars represent standard deviations (n=3), λ_{ex}=468 nm

(R^2 = 0.9951, 0.9923, respectively) between fluorescence intensity ratio (F/F_0) and the concentration of $Na_2S_2O_4$ (0～130 μmol/L). On the basis of the international union of pure and applied chemistry (IUPAC) recommendations, the detection limits for **Azo-BDP1** and **Azo-BDP2** were calculated to be 0.15 and 0.33 μmol/L, respectively. As show in Figure 1b, the absorption peak of **Azo-BDP1** at 398 nm was the characteristic absorption peak of azo group, while 591 nm was that of the BODIPY core. With the continuous adding of $Na_2S_2O_4$, the peaks at 398 and 591 nm disappeared gradually and an obviously absorption peak arose at 490 nm. These phenomena indicated that along with the increase concentration of $Na_2S_2O_4$, the structure of the azo group and BODIPY core had changed. This transformation attributed to the fact that azo group was reduced by $Na_2S_2O_4$ and the conjugate structure of styrene system was altered. At the same time, the appearance of new absorption at 490 nm illustrated the azo bond was reduced into amino-group. The reduction product of amino-group substituted BODIPY was confirmed by ESI-MS. The same process worked with **Azo-BDP2**, the absorption peaks of **Azo-BDP2** at 394 and 585 nm gradually disappeared with the increase of $Na_2S_2O_4$ concentration, and an obvious absorption peak appeared at 481 nm (Figure 1d). Appearance of a new blue shift absorption peak also proved that the azo bond of **Azo-BDP2** was reduced into NH_2 after the addition of $Na_2S_2O_4$.

To evaluate the response sensitivity, time-dependent fluorescence experiments was carried out. The result showed that **Azo-BDP1** and **Azo-BDP2** can completely react with $Na_2S_2O_4$ in a short time, while the response time of **Azo-BDP1** is faster than **Azo-BDP2** (Figures 2a and 2c). The time-dependent absorbance spectra of the reaction of $Na_2S_2O_4$ with **Azo-BDP1** and **Azo-BDP2** are shown in Figures 2b and 2d, which are similar to concentration-dependent absorbance spectra. **Azo-BDP1** exhibites the fastest response at 37 ℃, while **Azo-BDP2** presentes the fastest response at 32 ℃. Moreover, **Azo-BDP1** and **Azo-BDP2** also display large Stokes shift and deep-red to near-infrared launch. Therefore, these probes are more conducive to image $Na_2S_2O_4$ in complex organisms.

It is also important to discuss and verify the recognition mechanism of **Azo-BDP1** and **Azo-BDP2**. As is known to all, N=N bond was easily reduced by $Na_2S_2O_4$, so it was introduced as the reaction site in the initial design strategy. To test the reduction process, high-resolution mass spectra (HRMS) experiment was carried out to analyze the mixture solution of the **Azo-BDP1** and $Na_2S_2O_4$. As expected, the HRMS spectrum of protonated molecular presented a peak

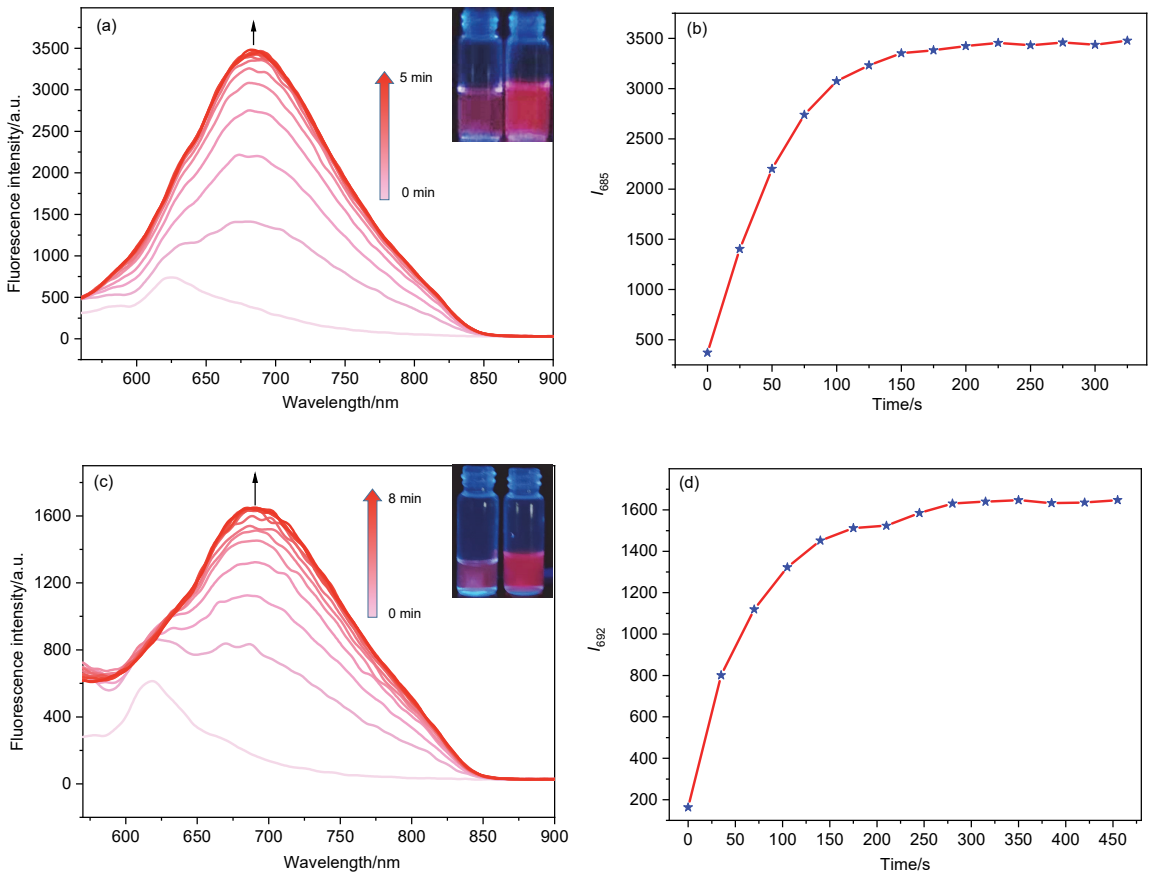

Figure 2 Time-dependent fluorescence spectra (a) and fluorescence intensity at 685 nm (b) of 10 μmol/L **Azo-BDP1** treated with 100 μmol/L $Na_2S_2O_4$ in DMSO solution; Time-dependent fluorescence spectra (c) and fluorescence intensity at 692 nm (d) of 10 μmol/L **Azo-BDP2** treated with 100 μmol/L $Na_2S_2O_4$ in DMSO solution

λ_{ex} = 468 nm. Error bars represent standard deviations (n = 3)

at *m*/*z* 578.194 corresponding to the molecular formula of $C_{30}H_{30}BF_2N_3O_4S$, which was belonged to a reduced product $[BDP\text{-}NH_2+H]^+$. Apparently, the results of HRMS experiment as well as the evidence of UV-vis absorption spectrum confirmed that the N=N bond of **Azo-BDP1** was reduced into NH_2 in the presence of $Na_2S_2O_4$, which fact reinforced our earlier design strategy.

Subsequently, the selectivity of **Azo-BDP1** and **Azo-BDP2** to $Na_2S_2O_4$ was evaluated in terms of sulfurcontaining species (Hcy, GSH, Cys, $Na_2S_2O_3$, Na_2SO_3, Na_2S, Na_2SO_4) and various bio-related substances (NaCl, $FeCl_2$, $NaNO_2$, NaBr, $CaCl_2$, $CuCl_2$, KI, $FeCl_3$, Vc, LT, *L*-Ser). As shown in Figures 3, S8 and S9, the probe gave obvious color enhancement effect and fluorescence enhancement with $Na_2S_2O_4$ while other tested species did not cause the same variation. Furthermore, competition experiments showed that in the presence of other competing substances, there was almost no interference in the response of **Azo-BDP1** and **Azo-BDP2**, therefore **Azo-BDP1** and **Azo-BDP2** could be used as a potential $Na_2S_2O_4$ probe in complex life forms.

2.3 Intravital imaging of **Azo-BDP1** in zebrafish embryos and zebrafish

Inspired by the favorable response of the probes to $Na_2S_2O_4$ *in vitro*, live zebrafish embryos were used to explore the imaging capabilities of **Azo-BDP1** for $Na_2S_2O_4$. As shown in Figure 4, using zebrafish embryos as a model for fluorescence microscope imaging experiments, zebrafish embryos gave weak red fluorescence signals after treating with 10 μmol/L **Azo-BDP1**. Opposite, when the zebrafish embryos containing **Azo-BDP1** was further incubated with $Na_2S_2O_4$ for 10 min, the fluorescence changed to a deep red fluorescent signal rapidly, indicating that the probe has favorable cell permeability and can quickly respond to $Na_2S_2O_4$ in zebrafish embryos.

To further explore the application of **Azo-BDP1** in living bodies, fluorescence imaging of zebrafish was performed. As shown in Figure 5, when the zebrafish incubated only with **Azo-BDP1** probe, the regions show a dull fluorescence, but a dull-to-bright transition of strong red fluorescence could be obtained in zebrafish once $Na_2S_2O_4$ was added. These findings indicate that the probe could be appropriately used for the detection of $Na_2S_2O_4$ *in vivo*.

3 Conclusions

In conclusion, aiming at the property of large Stokes shift and near infrared fluorescence, the BODIPY probes **Azo-**

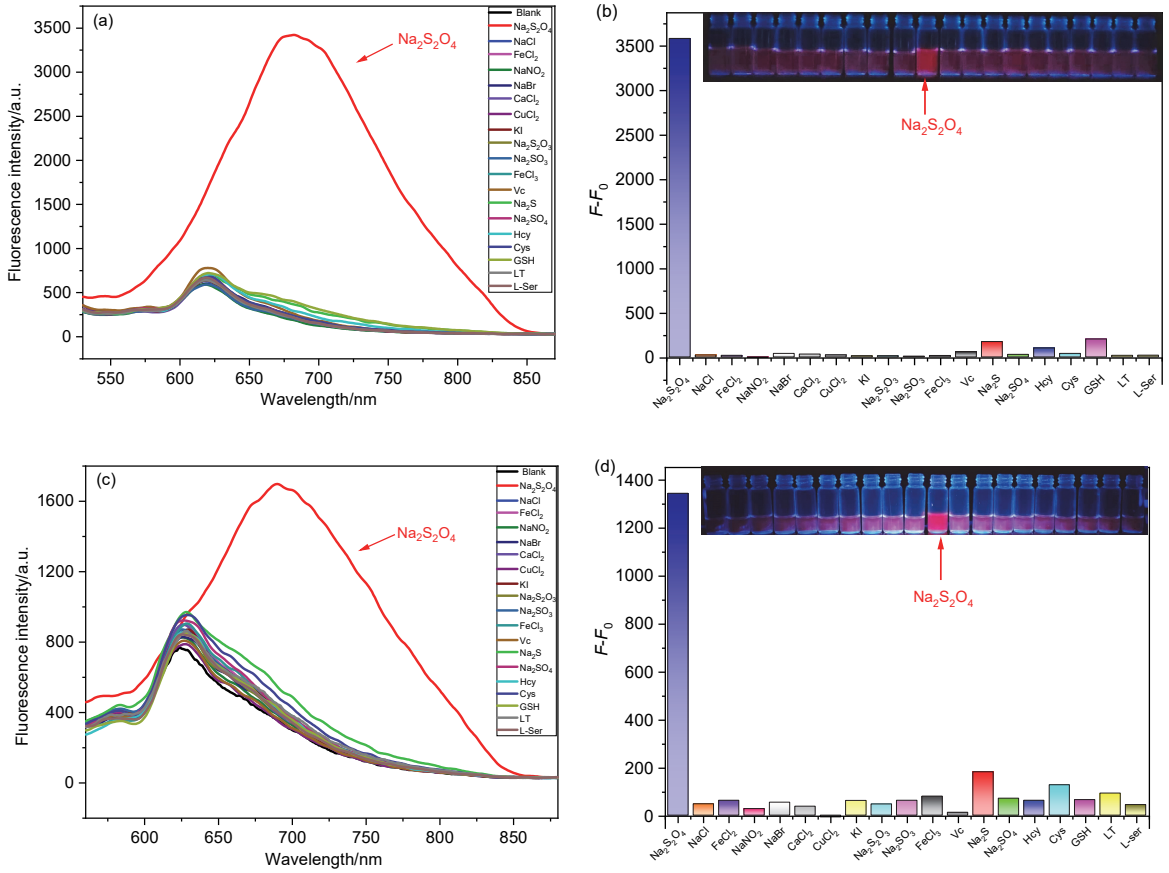

Figure 3 Fluorescence spectra (a) and fluorescence intensity ($F-F_0$) at 685 nm (b) of 10 μmol/L **Azo-BDPP1** treated with various species (inset: under irradiation at 365 nm of the probe **Azo-BDP1** with different compound); Fluorescence spectra (c) and fluorescence intensity ($F-F_0$) at 692 nm (d) of 10 μmol/L **Azo-BDP2** treated with various species (inset: under irradiation at 365 nm color change of the probe **Azo-BDP2** with different compound

$Na_2S_2O_4$, NaCl, $FeCl_2$, $NaNO_2$, NaBr, $CaCl_2$, $CuCl_2$, KI, $Na_2S_2O_3$, Na_2SO_3, $FeCl_3$, Vc, Na_2S, Na_2SO_4, Hcy, Cys, GSH, LT, *L*-Ser. λ_{ex}=468 nm

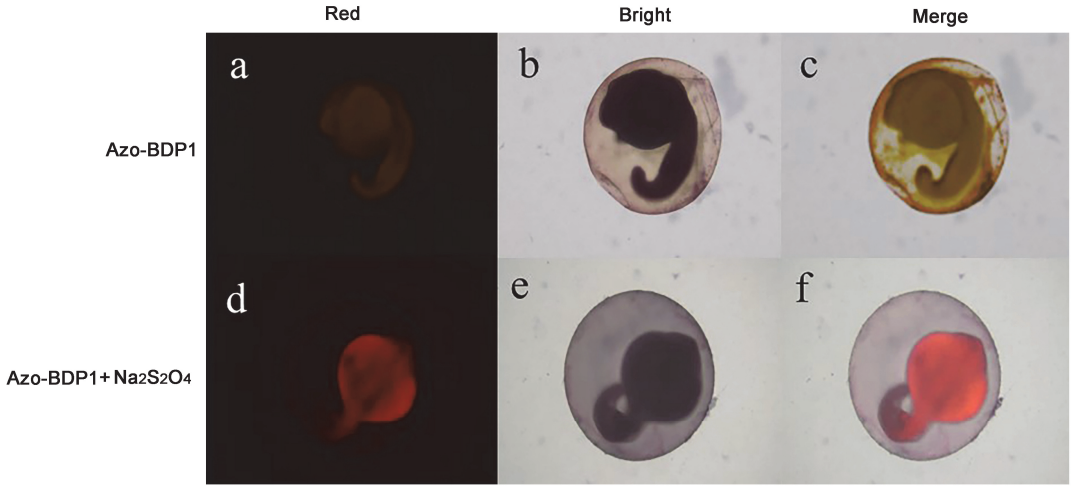

Figure 4 Images of live zebrafish embryos

(a) Fluorescent images of live zebrafish incubated with **Azo-BDP1** (10.0 μmol/L) for 10 min, (b) bright field, (c) merged images; (d) fluorescence image of living cells pretreated with **Azo-BDP1** (10.0 μmol/L) for 10 min and further incubated with $Na_2S_2O_4$ (100 μmol/L) for 10 min, (e) bright field, (f) merged images, λ_{ex}=525 nm

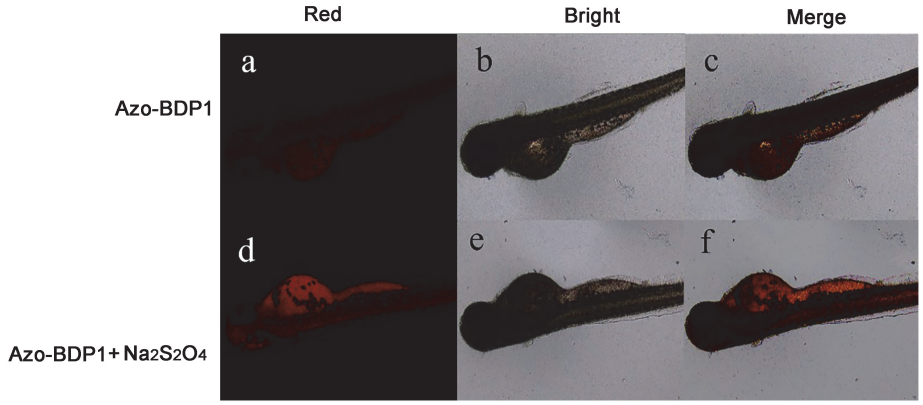

Figure 5 Images of live zebrafish

(a) Fluorescent images of live zebrafish incubated with **Azo-BDP1** (10.0 μmol/L) for 10 min, (b) bright field, (c) merged images; (d) fuorescence image of living cells pretreated with **Azo-BDP1** (10.0 μmol/L) for 10 min and further incubated with $Na_2S_2O_4$ (100 μmol/L) for 10 min, (e) bright field, (f) merged images, λ_{ex}=525 nm

BDP1 and **Azo-BDP2** for the determination of $Na_2S_2O_4$ were rationally designed and synthesized by Knoevenagel condensation. Based on the reaction recognition mechanism, the two probes included azo group as the response site and the BODIPY core as the fluorescent part. In the process of the detection of $Na_2S_2O_4$, fluorescent probes **Azo-BDP1** and **Azo-BDP2** exhibited special properties such as high selectivity, visualization, large Stokes shift and high sensitivity near infrared. Fluorescence imaging of zebrafish embryos and zebrafish further indicated that these probes can be used for the detection of $Na_2S_2O_4$, which is a substitute for azo reductase *in vitro*. Due to the recognition ability to azo reductase, **Azo-BDP1** and **Azo- BDP2** are expected to be used in the detection of early hypoxic tumor cells.

4 Experimental section

4.1 Materials and methods

All spectra were measured at room temperature (25 ℃). The ^{1}H NMR (600 MHz) spectra and ^{13}C NMR (150 MHz) spectra were recorded on an Agilent DD2 600 spectrometer with chemical shifts referenced to internal tetramethylsilane (TMS), and chemical shifts are reported relative to the solvent residue peaks ($CDCl_3$, δ 7.26 for ^{1}H NMR, δ 77.16 for ^{13}C NMR). High-resolution mass spectra (HRMS) were obtained from an Agilent 6510 Accurate-Mass Q-TOF LC/MS system. UV-Vis and fluorescent spectra were carried out on T6 ultraviolet-visible absorption spectrophotometer and F97pro fluorescence spectrophotometer, respectively. All reagents are purchased from reagent suppliers and used directly. The zebrafish embryos and zebrafish were imaged using a fluorescence microscope (Nikon, TS2-FL) and the excitation wavelength was 525 nm. Dry methylene chloride and triethylamine were obtained by reevaporation of calcium hydride. Solvents used in spectral measurement are all analytical grade. Pre-coated silica gel plate for TLC analysis and silica gel (200～300 mesh) for column chromatography were purchased from Qingdao Ocean Chemical. The UV absorption and fluo-

rescence spectra of **Azo-BDP1** and **Azo-BDP2** were tested in DMSO (10 μmol/L). **Azo-BDP1** and **Azo-BDP2** stock liquors (10 μmol/L) were prepared in THF. The following analytes were prepared in secondary deionized water (10 mmol): $Na_2S_2O_4$, NaCl, $FeCl_2$, $NaNO_2$, NaBr, $CaCl_2$, $CuCl_2$, KI, $Na_2S_2O_3$, Na_2SO_3, $FeCl_3$, Vc, Na_2S, Na_2SO_4, Hcy, Cys, GSH, LT, *L*-Ser.

4.2 Experimental method

4.2.1 Synthesis of **Ab**

Synthesis of **Ab** was carried out in a one-pot reaction according to the published method.[37] The mixture of NH_4Cl (0.53 g, 9.93 mmol) and *p*-nitrobenzaldehyde (1.00 g, 6.62 mmol) was added to a 250 mL round bottom flask containing 100 mL of MeOH, then reduced iron powder (1.48 g, 26.47 mmol) was added, and the mixture was stirred at reflux for 3 h. The crude product was filtered and concentrated under reduced pressure. The resulting solid was washed with water and dried to obtain a yellow solid (782.00 mg, 97%).

4.2.2 Synthesis of **Azo1**

4-Aminobenzaldehyde (0.36 g, 3.00 mmol) was added with 6 mL of 2 mol/L HCl and stirred at −5～0 ℃ for 5 min, then added saturated aqueous solution of $NaNO_2$ (0.23 g, 3.30 mmol) and continued to stir for 30 min. A cold solution of phenol (10% NaOH) was added dropwise to the above system and stirring was continued for 30 min at −10 ℃. The pH was adjusted until a large number of solids appeared. The solids were filtered and washed with water, and then dried to obtain an orange-yellow solid **Azo1** (560.00 mg, 82%). ^{1}H NMR (400 MHz, DMSO-d_6) δ: 10.52 (s, 1H), 10.06 (s, 1H), 8.09～8.01 (m, 2H), 7.94 (d, J=8.4 Hz, 2H), 7.88～7.80 (m, 2H), 6.99～6.91 (m, 2H); ^{13}C NMR (151 MHz, DMSO-d_6) δ: 193.0, 162.3, 155.3, 145.8, 137.2, 131.2, 125.9, 123.1, 116.6. HRMS (ESI) calcd for $C_{13}H_{11}N_2O_2$ $[M+H]^+$ 227.0821, found 227.0823.

4.2.3 Synthesis of **Azo2**

The mixture of compound **Ab2** (1.00 g, 4.42 mmol) and K_2CO_3 (0.92 g, 6.63 mmol) was added to a solution of dry acetone (40 mL), MOMCl (0.53 g, 6.63 mmol) was added under argon protection and the mixture was stirred at room temperature for 12 h. The crude product was concentrated under reduced pressure and purified by silica gel flash column chromatography (silica gel, *V*(petroleum ether)∶*V*(ethyl acetate)=4∶1) to obtain an orange-yellow solid **Azo2** (1.12 g, 94%).^{1}H NMR (600 MHz, $CDCl_3$) δ: 10.09 (s, 1H), 8.01 (d, J=3.1 Hz, 4H), 7.95 (d, J=9.0 Hz, 2H), 7.17 (d, J=9.0 Hz, 2H), 5.27 (s, 2H), 3.51 (s, 3H); ^{13}C NMR (151 MHz, $CDCl_3$) δ: 191.6, 160.4, 156.1, 147.6, 137.0, 130.7, 130.6, 125.2, 123.7, 123.1, 116.4, 96.1, 94.3, 56.3. HRMS (ESI) calcd for $C_{15}H_{15}N_2O_3$ $[M+H]^+$ 271.1083, found 271.1087.

4.2.4 Synthesis of **BDP**

The mixture of 2,4-dimethyl-1*H*-pyrrole-3-carboxylic acid ethyl ester (0.67 g, 4.00 mmol) and 2-thiophenecarboxaldehyde (0.23 g, 2.00 mmol) was added to dry dichloromethane (100 mL), *p*-TsOH (0.10 mmol, 17.22 mg) was add to solution and TLC detects that the reaction of the raw materials is complete. then 2,3-dichloro-5,6-dicyano-1,4-benzoquinone (DDQ, 0.45 g, 2.00 mmol) was added, and stirred under the flow of Ar gas. After 1 h, Et_3N (3 mL) and BF_3OEt_2 (4 mL) were added to the solution and stirred for 5 h. After the reaction was completed, saturated $NaHCO_3$ was added to quench the reaction. The organic phase was washed three times with brine, dried with Na_2SO_4, and then concentrated under reduced pressure. The obtained mixture was purified by silica gel flash column chromatography (silica gel, *V*(petroleum ether)∶ *V*(ethyl acetate)=8∶1) to obtain red crystals of **BDP** (680.00 mg, yield 72%). ^{1}H NMR (600 MHz, $CDCl_3$) δ: 7.58 (dd, J=5.0, 1.2 Hz, 1H), 7.18 (dd, J=5.1, 3.5 Hz, 1H), 7.01 (dd, J=3.5, 1.2 Hz, 1H), 4.28 (q, J=7.1 Hz, 4H), 2.85 (s, 6H), 1.85 (s, 6H), 1.33 (t, J=7.1 Hz, 6H); ^{13}C NMR (150 MHz, $CDCl_3$) δ: 164.1, 150.0, 148.9, 138.2, 133.93, 132.3, 128.4, 128.3, 128.1, 122.8, 60.3, 15.0, 15.0, 15.0, 14.3, 12.8. HRMS (ESI) calcd for $C_{23}H_{26}BF_2N_2O_4S$ $[M+H]^+$ 475.1675, found 475.1692.

4.2.5 Synthesis of **Azo-BDP1**

A mixture of 15 mL of toluene, **BDP** (95.00 mg, 0.20 mmol), **Azo1** (68.00 mg, 0.30 mmol), CH_3COOH (0.2 mL) and piperidine (0.2 mL) was added to a 50 mL round-bottom flask and stirred at reflux for 12 h. After the reaction, the reaction was quenched by distilled water and the organic phase was extracted three times with CH_2Cl_2, then dried over Na_2SO_4 and concentrated under reduced pressure. The obtained mixture was purified by silica gel flash column chromatography (silica gel, *V*(petroleum ether)∶ *V*(ethyl acetate)=8∶1) to obtain black crystals of **Azo-BDP1** (21.0 mg, yield 15%). ^{1}H NMR (400 MHz, $CDCl_3$) δ: 12.21 (s, 1H), 7.91～7.89 (m, 4H), 7.69～7.67 (m, 3H), 7.40 (d, J=1.7 Hz, 1H), 6.98 (d, J=2.8 Hz, 1H), 6.89～6.82 (m, 4H), 4.32 (q, J=7.1 Hz, 4H), 2.81 (s, 3H), 1.81 (s, 3H), 1.69 (s, 3H), 1.36～1.28 (m, 6H); ^{13}C NMR (151 MHz, $CDCl_3$) δ: 173.6, 169.9, 164.8, 158.7, 148.7, 143.4, 142.2, 138.4, 130.4, 130.2, 129.9, 128.5, 127.5, 122.9, 116.4, 115.3, 62.4, 61.2, 60.4, 29.7, 16.6, 14.4, 14.3, 11.9, 11.8. HRMS (ESI) calcd for $C_{36}H_{34}BF_2N_4O_5S$ $[M+H]^+$ 683.2312, found 683.2319.

4.2.6 Synthesis of **Azo-BDP2**

The synthesis method of **Azo-BDP2** is similar to **Azo-BDP1**. 27.00 mg, yield 18%. ^{1}H NMR (400 MHz, $CDCl_3$) δ: 7.97～7.89 (m, 4H), 7.77～7.69 (m, 3H), 7.61～7.90 (m, 1H), 7.42 (d, J=16.6 Hz, 1H), 7.22～7.14 (m, 3H), 7.05 (d, J=4.5 Hz, 1H), 5.27 (s, 2H), 4.37～4.27 (m, 4H), 2.88 (s, 3H), 1.88 (s, 3H), 1.75 (s, 3H), 1.36～1.29 (m, 6H); ^{13}C NMR (151 MHz, $CDCl_3$) δ: 165.4, 164.1, 159.8, 152.9, 147.8, 139.2, 138.5, 134.0, 128.5, 128.4, 128.1, 124.8, 123.2, 116.4, 96.1, 94.3, 61.1, 60.3, 56.2, 29.4, 15.2, 14.3, 14.2, 12.9, 12.4. HRMS (ESI) calcd for $C_{38}H_{38}BF_2N_4O_6S$ $[M+H]^+$ 727.2574, found 727.2585.

Supporting Information UV-vis and fluorescence spectra of probes **Azo-BDP1** and **Azo-BDP2**. ^{1}H NMR, ^{13}C NMR and MS spectra of **Azo-BDP1** and **Azo-BDP2**. The Supporting Information is available free of charge via the Internet at http://sioc-journal.cn/.

References

[1] Henry, A. *J. Chem. Educ*. **1996**, 1068.
[2] Skypala, I. J.; Williams, M.; Reeves, L.; Meyer, R.; Venter, C. *Clin. Transl. Allergy* **2015**, *5*, 2.
[3] Xue, T.; Shen, J.; Shao, K.; Wang, W.; Wu, B.; He, Y. *Chem. Eur. J.* **2020**, *26*, 2521.
[4] Huang, J.; Wu, Y.; Zeng, F.; Wu, S. *Theranostics* **2019**, *9*, 7313.
[5] Wang, C.; Zhang, S.; Huang, J.; Cui, L.; Hu, J.; Tan, S. *RSC Adv*. **2019**, *9*, 21572.
[6] Cai, Q.; Yu, T.; Zhu, W.; Xu, Y.; Qian, X. *Chem. Commun*. **2015**, *51*, 14739.
[7] Piao, W.; Tsuda, S.; Tanaka, Y.; Maeda, S.; Liu, F.; Takahashi, S.; Kushida, Y.; Komatsu, T.; Ueno, T.; Terai, T.; Nakazawa, T.; Uchiyama, M.; Morokuma, K.; Nagano, T.; Hanaoka, K. *Angew. Chem., Int. Ed*. **2013**, *52*, 13028.
[8] Tan, J. W.; Tham, C. L.; Israf, D. A. *Neurochem. Res*. **2013**, *38*, 512.
[9] Yu, X.; Xiang, L.; Yang, S., Qu, S.; Zeng, X.; Zhou, Y.; Yang, R. *Spectrochim. Acta A* **2020**, *245*, 118887.
[10] Ruan, S.; Zhang, Y.; Wu, S.; Gao, Y.; Yang, L.; Li, M.; Yang, Y.; Wang, Z.; Wang, S. *Inorg. Chem. Commun.* **2021**,*132*, 108847.
[11] Feng, G.; Luo, C.; Yi, H.; Yuan, L.; Lin, B.; Luo, X.; Hu, X.; Wang, H.; Lei, C.; Nie, Z.; Yao, S. *Nucleic Acids Res.* **2017**, *45*, 10380.
[12] He, R.; Zhang, Y.; Madhu, S.; Gao, Q.; Lian, Q.; Raghavan, S. S.; Geng, J. *Chem. Commun.* **2020**, *56*, 14717.
[13] Ren, X.; Liao, L.; Yang, Z.; Li, H.; Li, X.; Wang, Y.; Ye, Y.; Song, X. *Chin. Chem. Lett.* **2021**, *32*, 1061.
[14] Li, J.-X.; He, R.-Y.; Duan, S.-L.; Li, J.-H.; Han, X.-J.; Ye, Y. *Chin. J. Org. Chem*. **2022**, *42*, 2428 (in Chinese).
(李嘉欣, 贺如艳, 段森林, 黎锦华, 韩校净, 叶勇, 有机化学, **2022**, *42*, 2428.)
[15] Jalalvand, A. R.; Goicoechea, H. C.; Gu, H. W. *Microchem. J*. **2019**, *144*, 6.
[16] Yu, X.; Xiang, L.; Yang, S.; Qu, S.; Zeng, X.; Zhou, Y.; Yang, R. *Spectrochim. Acta*, *Part A* **2021**, *245*, 118887.
[17] Dong, B.; Song, W.; Kong, X.; Zhang, N.; Lin, W. *J. Mater. Chem. B* **2019**, *7*, 730.
[18] Q. L.; Yan, C.; Zhang, J.; Guo, Z.; Zhu, W. H. *Dyes Pigm*. **2019**, *162*, 802.
[19] Feng, G.; Luo, C.; Yi, H.; Yuan, L.; Lin, B.; Luo, X.; Hu, X.; Wang, H.; Le, C.; Nie, Z.; Yao, S. *Nucleic Acids Res*. **2017**, *45*, 10380.
[20] Chen, J. B.; Zhang, H. X.; Guo, X. F.; Wang, H.; Zhang, H. S. *Anal. Bioanal. Chem*. **2013**, *405*, 7447.
[21] Zhao, X.; Li, N.; Liu, F.; Gao, C.; Feng, J.; Liu, L.; Guan, X.; Yan, N. *J. Org. Chem.* **2020**, *40*, 4339.
[22] Dzyuba, S. V. *Biosensors* **2020**, *10*, 192.
[23] Li, L.; Dong, X.; Li, J.; Wei, J. *Dyes Pigm.* **2020**, *183*, 108756.
[24] Singh, S. P.; Gayathri, T. *Eur. J. Org. Chem*. **2014**, *2014*, 4689.
[25] Song, X.; Xu, Y.; Tao, X.; Gao, X.; Wu, Y.; Yu, R.; He, Y.; Tao, Y. *Macromol. Rapid Commun*. **2022**, 2100828.
[26] Shi, Z.; Han, X.; Hu, W.; Bai, H.; Peng, B.; Ji, L.; Fan, Q.; Li, L.; Huang, W. *Chem. Soc. Rev*. **2020**, *49*, 7533.
[27] Zhu, X. Y.; Yao, H. W.; Fu, Y. J.; Guo, X. F.; Wang, H. *Anal. Chim. Acta* **2019**, *1048*, 194.
[28] Xu, Z.; Song, A.; Wang, F.; Chen, H. *RSC Adv*. **2021**, *11*, 32203.
[29] Yao, C.; Chen, Y.; Zhao, M.; Wang, S.; Wu, B.; Yang, Y.; Yin, D.; Yu, P.; Zhang, H.; Zhang, F. *Angew. Chem., Int. Ed*. **2022**, *61*, e202114273.
[30] Yang, L.; Liu, Y.; Ma, C.; Liu, W.; Li, Y.; Li, L. *Dyes Pigm.* **2015**, *122*, 1.
[31] Zhao, X.; Gao, C.; Li, N.; Liu, F.; Huo, S.; Li, J.; Guan, X.; Yan, N. *Tetrahedron Lett*. **2019**, *60*, 1452.
[32] Ahmed, N.; Zareen, W.; Ye, Y. *Chin. Chem. Lett.* **2022**, *33*, 2765.
[33] Zhu, S.; Zhang, J.; Vegesna, G.; Tiwari, A.; Luo, F. T.; Zeller, M.; Luck, R.; Li, H.; Green, S.; Liu, H. *RSC Adv*. **2012**, *2*, 404.
[34] Zou, J.; Wang, P.; Wang, Y.; Liu, G.; Zhang, Y.; Zhang, Q.; Shao, J.; Si, W.; Huang, W.; Dong, X. *Chem. Sci*. **2019**, *10*, 268.
[35] Zhang, X.; Xiao, Y.; Qi, J.; Qu, J.; Kim, B.; Yue, X.; Belfield, K. D. *J. Org. Chem*. **2013**, *78*, 9153.
[36] Kang, J.; Huo, F.; Ning, P.; Meng, X.; Chao, J.; Yin, C. *Sens. Actuators B Chem*. **2017**, *250*, 342.
[37] Baker, J. R.; Gilbert, J.; Paula, S.; Zhu, X.; Sakoff, J. A.; McCluskey, A. *ChemMedChem* **2018**, *13*, 1447.

(Lu, Y.)

